JACS Au
AN OPEN ACCESS JOURNAL OF THE AMERICAN CHEMICAL SOCIETY

pubs.acs.org/jacsau
Article

$_{CG}$-SLENP: A Chemical Genetics Strategy To Selectively Label Existing Proteins and Newly Synthesized Proteins

Jian Wang, Bo Chao, Jake Piesner, Felice Kelly, Stefanie Kaech Petrie, Xiangshu Xiao, and Bingbing X. Li*

Cite This: JACS Au 2024, 4, 3146−3156
Read Online

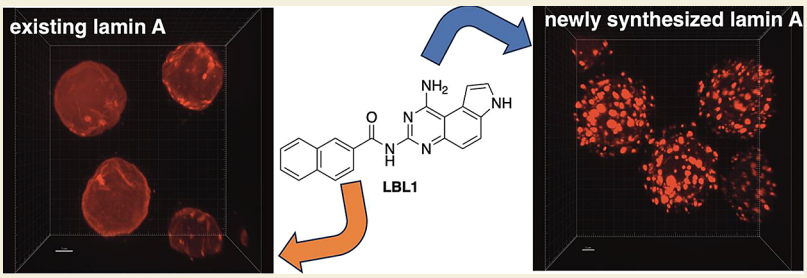

ABSTRACT: Protein synthesis and subsequent delivery to the target locations in cells are essential for their proper functions. Methods to label and distinguish newly synthesized proteins from existing ones are critical to assess their differential properties, but such methods are lacking. We describe the first chemical genetics-based approach for selective labeling of existing and newly synthesized proteins that we termed as $_{CG}$-SLENP. Using HaloTag in-frame fusion with lamin A (LA), we demonstrate that the two pools of proteins can be selectively labeled using $_{CG}$-SLENP in living cells. We further employ our recently developed selective small molecule ligand **LBL1** for LA to probe the potential differences between newly synthesized and existing LA. Our results show that **LBL1** can differentially modulate these two pools of LA. These results indicate that the assembly states of newly synthesized LA are distinct from existing LA in living cells. The $_{CG}$-SLENP method is potentially generalizable to study any cellular proteins.

KEYWORDS: *lamin, LBL1, newly synthesized protein, existing protein, HaloTag, chemical genetics, labeling*

INTRODUCTION

Cellular protein synthesis is essential for protein homeostasis and life. Once proteins are synthesized at the ribosomes, they undergo different post-translational modifications and trafficking processes to reach their target destinations to execute their functions in cells. Almost all proteins in cells execute their functions through formation of specialized multimeric complexes.[1] One mechanism for the formation of multimeric protein complexes is through random or directed collision to form complexes once the protein subunits are fully synthesized and released from the ribosomes. Alternatively and perhaps more likely, the protein subunits are folded and the protein complexes are formed while they are being translated at the ribosomes.[2,3] This so-called cotranslational assembly mechanism offers potential benefits of stabilizing nascent polypeptide chains and preventing formation of toxic polypeptides, which in turn facilitates the requisite complex formation.[2,4] However, the nature and properties of newly formed complexes in cells are largely unknown partly due to the significant challenges associated with identifying, isolating, and characterizing these complexes in cells.

Mammalian cells have an intricate network of proteins that form the cytoskeleton. These include microtubules, actin filaments, and various intermediate filaments (IF).[5] Among the IF proteins, nuclear lamins are type V IF proteins localized underneath the inner nuclear membrane (INM).[6] In mammalian cells, three lamin genes lamin A, B1, and B2 (LMNA, LMNB1, and LMNB2) encode four major lamin proteins: lamin A (LA), lamin B1 (LB1), lamin B2 (LB2), and lamin C (LC) that form the proteinaceous meshwork underneath INM.[7] All the lamin proteins contain an *N*-terminal nonhelical head domain, a central long coiled-coil domain, a nuclear localization sequence (NLS), and a C-terminal globular immunoglobulin (Ig) fold.[8] Through the central coiled-coil domain, lamins form dimers that are further assembled into long filaments with the originally estimated diameter of ∼10 nm.[9] More recent cryo-electron tomography (cryo-ET) studies indicated that the diameter of lamins in

Received: May 29, 2024
Revised: June 26, 2024
Accepted: June 27, 2024
Published: July 25, 2024

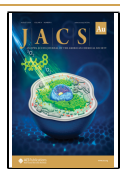

https://doi.org/10.1021/jacsau.4c00461
JACS Au 2024, 4, 3146−3156

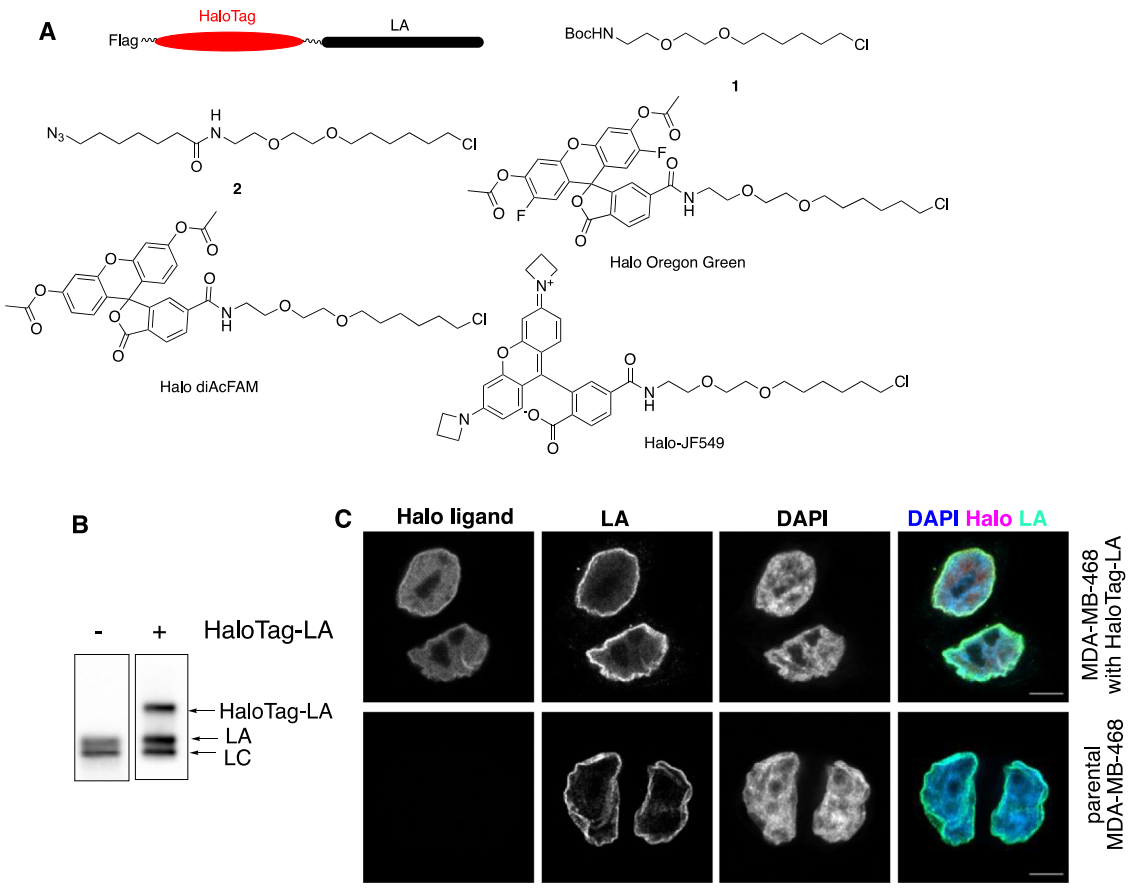

Figure 1. HaloTag-LA was stably expressed in MDA-MB-468 cells. (A) Schematic drawing of Flag-HaloTag-LA fusion (see Figure S1 for sequence). Chemical structures of masking halo ligand **1**, clickable halo ligand **2** and other fluorescent Halo ligands used are shown. (B) HaloTag-LA was expressed in MDA-MB-468 cells. The crude cell lysates from parental cells and the cells with lentiviral expression were prepared for Western blot analysis and blotted with anti-LA. (C) HaloTag-LA fusion was stably integrated into nuclear lamina. The parental MDA-MB-468 cells and their counterparts expressing HaloTag-LA were treated with Halo-JF549. The cells were also costained with anti-LA while the nucleus was stained with DAPI. The confocal micrographs of representative cells are shown. Scale bars are 5 μm.

somatic cells is ~3.5 nm, which is significantly smaller than that initially estimated.[10,11]

As a nuclear protein, LA is synthesized in the cytosol and then translocated into the nucleus to be facilitated by the NLS in LA using nuclear importin receptors.[12] Many nuclear proteins including nuclear transcription complexes and nuclear pore complexes have been reported to undergo cotranslational complex formation for subsequent nuclear translocation.[13,14] It has also been suggested that LA is dimerized in the cytosol either as a homodimer or heterodimer for subsequent nuclear translocation.[12] However, the nature of the higher-order structures of newly synthesized LA relative to existing LA in the nuclear envelope is unknown. In this study, we designed the $_{CG}$-SLENP strategy to distinguish the newly synthesized LA from existing LA. We further employed small molecule ligand **LBL1** to evaluate its effect on the dynamics of newly synthesized and existing LA pools using $_{CG}$-SLENP, providing fresh insights into the assembly states of LA in cells. **LBL1** is the first small molecule ligand known to selectively bind to nuclear lamins and it can stabilize the oligomeric state of LA.[15,16]

RESULTS AND DISCUSSION

Design of $_{CG}$-SLENP Using HaloTag and Halo Ligands

In order to investigate the nature of newly synthesized proteins, we would need a SLENP method to distinguish this population from the existing counterpart. Previously described metabolic labeling methods using radioactive amino acids or bioorthogonally modified amino acids[17,18] can lead to identification of newly synthesized species, but not the existing ones. This metabolic labeling approach also involves laborious downstream procedures including immunoprecipitation to identify the specific protein of interest. To circumvent these issues, we developed a chemical genetics strategy with the goal to selectively label newly synthesized and existing proteins. Using LA as an example, our $_{CG}$-SLENP strategy is depicted in Figures 1 and 2. We envisioned that expression of HaloTag-LA fusion in cells would help distinguish the two populations using different chloroalkane ligands. HaloTag is an engineered bacterial dehalogenase that covalently reacts with chloroalkane compounds, which are collectively called halo ligands.[19] We hypothesized that upon reacting with a silent halo ligand to exhaust existing HaloTag-LA fusion, the newly synthesized HaloTag-LA can be labeled by an orthogonal halo ligand to effectively distinguish the two populations (Figure 2A). Thus, a lentiviral construct expressing HaloTag protein in-frame with LA fusion was created and

https://doi.org/10.1021/jacsau.4c00461
JACS Au 2024, 4, 3146−3156

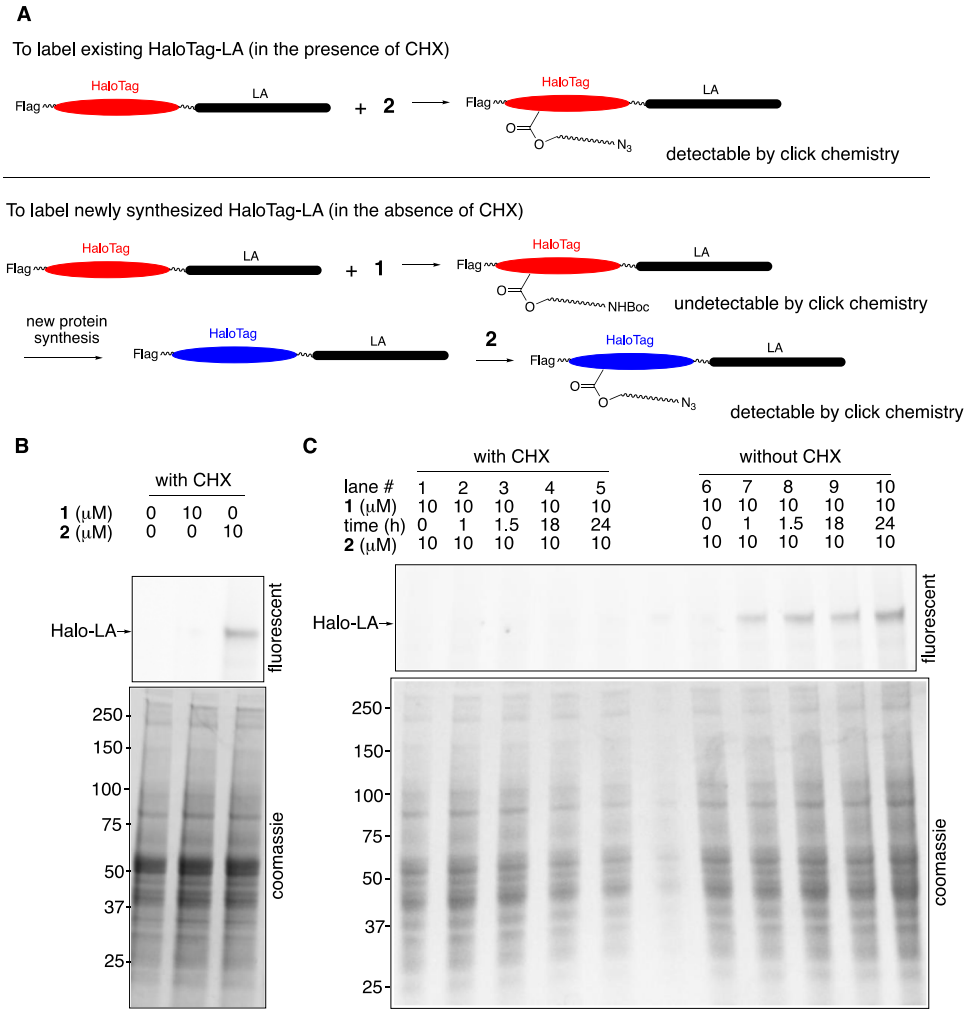

Figure 2. $_{CG}$-SLENP to distinguish existing HaloTag-LA and newly synthesized HaloTag-LA. (A) Schematic diagrams to illustrate the $_{CG}$-SLENP strategy to label existing HaloTag-LA (top) and newly synthesized HaloTag-LA (bottom). (B) MDA-MB-468 cells expressing HaloTag-LA were treated with CHX along with compound **1** for 30 min. Then the media were removed and fresh media containing CHX and compound **2** (10 μM) were added and incubated for 30 min. The cells were harvested and the lysates were prepared for click reaction with TAMRA-alkyne. The resulting lysates were separated on a SDS-PAGE gel and the gel was fluorescently imaged (top). The gel was then stained with Coomassie blue (bottom) as a loading control. (C) MDA-MB-468 cells expressing HaloTag-LA were treated with CHX (0 or 0.1 mg/mL) along with compound **1** for 30 min. Then the media were removed and fresh media containing CHX (0 or 0.1 mg/mL) were added for the indicated time duration, when compound **2** (10 μM) was added and incubated for 30 min. The cells were harvested, and the lysates were prepared for click reaction with TAMRA-alkyne. The resulting lysates were separated on a SDS-PAGE gel and the gel was fluorescently imaged (top). The gel was then stained with Coomassie blue (bottom) as a loading control.

Scheme 1. Synthesis of Halo Ligands 1 and 2

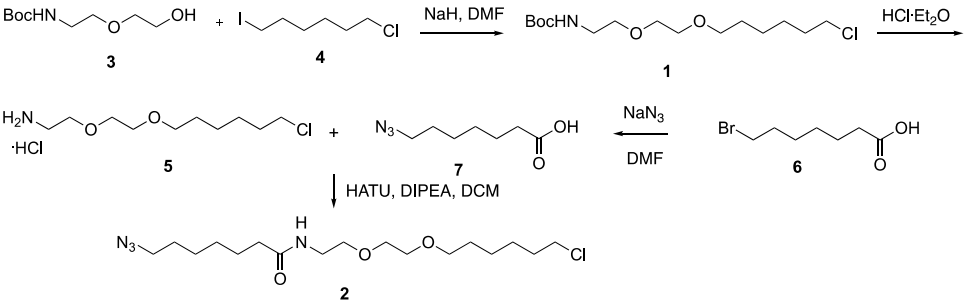

sequence verified (see Figure S1 for sequence). This construct was then stably expressed in MDA-MB-468 cells using lentiviruses. As shown in Figure 1B, the fusion was expressed in cells at a similar level to the endogenous LA protein. As reported before by us and others in different cell types,[15,20] endogenous LA was stably integrated into nuclear lamina underneath INM in MDA-MB-468 cells (Figure 1C, bottom). At the same time, a fraction of LA was also detected in the nucleoplasm. To examine if exogenously expressed HaloTag-LA was also integrated into the nuclear lamina, we treated

https://doi.org/10.1021/jacsau.4c00461
JACS Au 2024, 4, 3146−3156

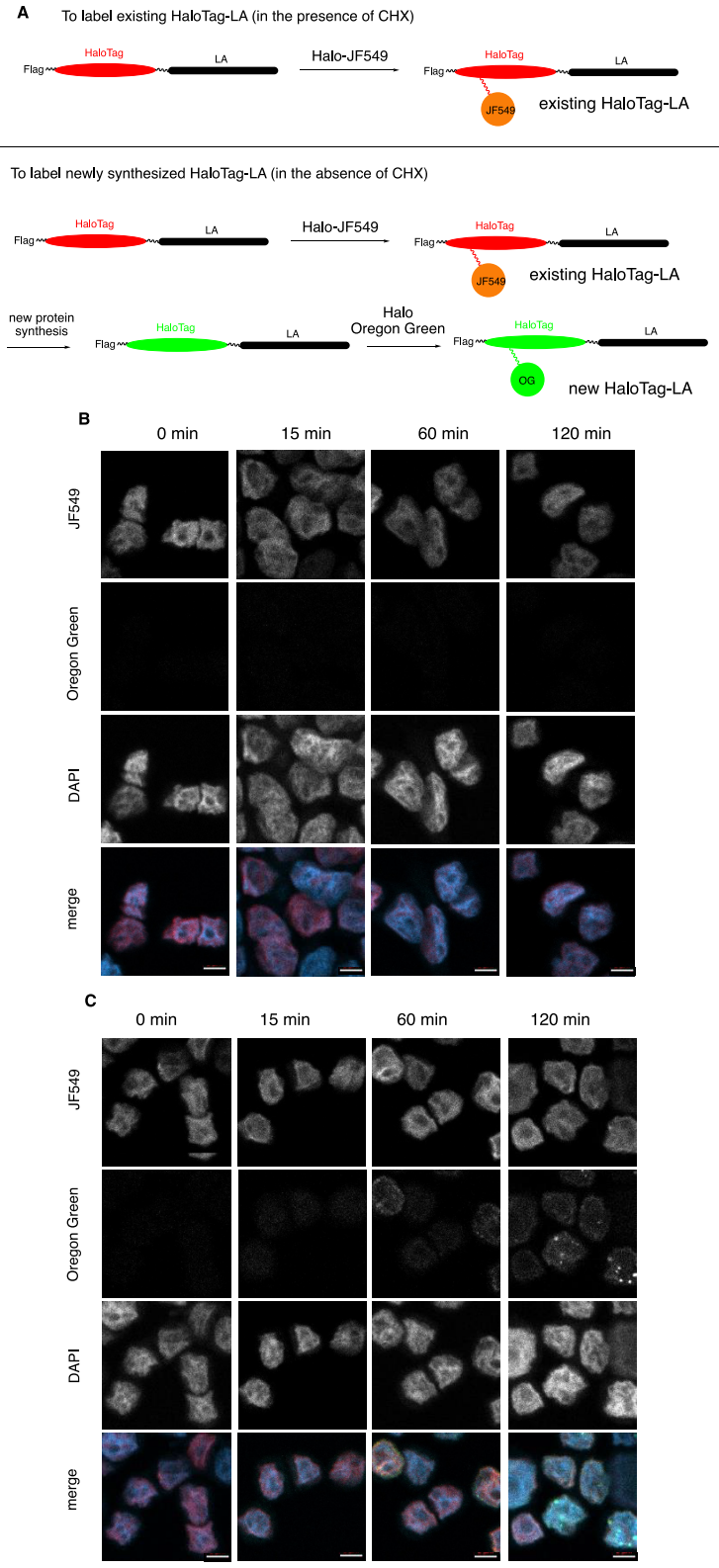

Figure 3. $_{CG}$-SLENP to dually label existing HaloTag-LA and newly synthesized HaloTag-LA in MDA-MB-468 cells. (A) Schematic diagram to illustrate dual labeling strategy for existing HaloTag-LA and newly synthesized HaloTag-LA using two different fluorescence Halo ligands. (B) Labeling of existing HaloTag-LA. The cells were treated with CHX and Halo-JF549. At different time point post Halo-JF549 labeling, the cells were further treated with Halo Oregon Green. The cell nucleus was counterstained with DAPI. (C) Dual labeling of existing HaloTag-LA and newly synthesized HaloTag-LA. The cells were first treated with Halo-JF549 without CHX. At the indicated time point post Halo-JF549 labeling, the cells were further treated with Halo Oregon Green. The cells were examined under a confocal microscope after the nucleus was counterstained with DAPI. The scale bars are 5 μm.

https://doi.org/10.1021/jacsau.4c00461
JACS Au 2024, 4, 3146−3156

MDA-MB-468 cells expressing HaloTag-LA with a fluorescent Janelia Fluor Halo ligand (Halo-JF549) (Figure 1A). The cells were also costained with anti-LA. As shown in Figure 1C (top), the Halo ligand signal was very similar to the LA signal in cells. We did, however, observe more nucleoplasmic LA signals in these cells, compared to parental cells. Treating the parental cells with Halo-JF549 did not generate any fluorescent signal (Figure 1C, bottom), supporting the specificity of the Halo ligand. For both parental and HaloTag-LA-expressing cells, there existed cell-to-cell heterogeneity of LA staining pattern and intensity (Figure S2). Similar heterogeneity was also observed in other cell types.[21,22]

With this unique HaloTag-LA system established, we interrogated the possibility to selectively detect the existing HaloTag-LA and newly synthesized HaloTag-LA. To distinguish these two populations, two different Halo ligands **1** and **2** were designed (Figures 1A and 2A). Ligand **1** was designed as a masking Halo ligand while **2** was designed as a reporting ligand by utilizing the built-in bioorthogonally reactive N_3 group, which can be detected by Cu(I)-catalyzed azide-alkyne cycloaddition reaction (aka click reaction) with a tagged alkyne.[23] The synthesis of these ligands is shown in Scheme 1 and was adapted from a previously reported synthesis.[24] Briefly, the Boc-protected alcohol **3** was alkylated with 1-chloro-6-iodohexane (**4**) in the presence of NaH to give Halo ligand **1**. The Boc group in **1** was deprotected under acidic conditions ($HCl{\cdot}E_2O$) to generate amine **5**, which was further coupled with azido acid **7** to be prepared from bromo acid **6** to furnish the desired Halo ligand **2**.

Selective Labeling of Newly Synthesized HaloTag-LA and Existing HaloTag-LA Using $_{CG}$-SLENP

With these two different Halo ligands in hand, we envisioned that existing HaloTag-LA would be labeled by Halo ligand **2** in the presence of a protein synthesis inhibitor cycloheximide (CHX)[25] to block new protein synthesis (Figure 2A). On the other hand, newly synthesized HaloTag-LA would be selectively labeled by first masking the existing HaloTag-LA using silent Halo ligand **1**, followed by chasing the newly synthesized HaloTag-LA using Halo ligand **2**. Once the newly synthesized HaloTag-LA is labeled by **2**, it can be visualized by a click reaction with a fluorescent alkyne (Figure 2A). To test this strategy, MDA-MB-468 cells expressing HaloTag-LA were treated with CHX, and then, the cells were labeled with **2** (10 μM) for 30 min. The cells were harvested and the lysates were prepared for a click reaction with a tetramethylrhodamine (TAMRA) conjugated terminal alkyne in the presence of TCEP, TBTA, and $CuSO_4$.[26] Then, the lysates were separated on an SDS-PAGE, and the gel was directly visualized by in-gel fluorescence scanning. As shown in Figure 2B, treatment with **2** resulted in specific and prominent labeling of HaloTag-LA. On the other hand, treatment of the cells with the masking ligand **1** (10 μM) did not produce any signal. Pretreatment of the cells with **1** followed by labeling with **2** in the presence of CHX also produced no labeling of HaloTag-LA (Figure 2C, lanes 1−5), indicating complete saturation of existing Halo-binding sites by **1** and no new HaloTag-LA was being synthesized under these conditions. When CHX was omitted from the treatment, we observed gradually increased labeling of HaloTag-LA when the cells were pretreated with **1** followed by a chasing period of **2** (lanes 6−10). Prominent labeling of HaloTag-LA was observed even 1 h after the existing HaloTag-LA was masked by ligand **1**, suggesting that HaloTag-LA is constantly being made in the cells. The labeling of newly synthesized HaloTag-LA was increased with longer chasing periods (Figure 2C, lanes 6−10). Similar protein loading in each lane was verified by Coomassie blue staining (Figure 2B, C). Because HaloTag-LA is integrated into the nuclear lamina as filaments, it is possible that a fraction of the Halo ligand binding site was not accessible when the cells were treated with **1**. During the subsequent period of time of labeling by **2**, the HaloTag-LA filaments might be dynamically rearranged to expose the unoccupied Halo ligand binding site, which would phenotypically produce the same results even in the absence of new protein synthesis. In this case, this alternative seems unlikely because when the cells were cotreated with CHX, no additional labeling of HaloTag-LA was observed during the subsequent treatment period of time (Figure 2C, lanes 1−5). Thus, the labeling seen with the sequential treatment of **1** and **2** indeed reported newly synthesized HaloTag-LA. These results also suggest that the existing HaloTag-LA filaments may not undergo dynamic structural remodeling or the Halo-binding site was fully exposed for labeling by ligand **1** during the masking period. To further support the former case, we employed fluorescence recovery after photobleaching (FRAP) to analyze the dynamics of HaloTag-LA. As shown in Figure S3, the existing HaloTag-LA labeled with Halo diAcFAM (Figure 1A) was not mobile. These results are consistent with previous FRAP studies with GFP-LA in different cell types to indicate that LA in the interphase is relatively immobile,[27] which is also consistent with our live cell imaging results (vide infra).

Dual Labeling of Newly Synthesized HaloTag-LA and Existing HaloTag-LA

To further evaluate the labeling of existing and newly synthesized HaloTag-LA, we investigated the feasibility of dual-labeling and visualization using different fluorescent Halo ligands (Figure 3A). To label existing HaloTag-LA, we treated cells with CHX to stop new protein synthesis and HaloTag-LA was labeled with Halo-JF549 (Figure 1A) for 30 min. At different periods post Halo-JF549 labeling, the cells were further treated with another fluorescent Halo ligand, Halo Oregon Green (Figure 1A). As shown in Figure 3B, the existing HaloTag-LA was efficiently labeled and visualized by Halo-JF549. Under this condition with CHX treatment, no Oregon Green signal was observed, indicating that the existing HaloTag-LA was fully labeled by Halo-JF549 and no new HaloTag-LA was being synthesized. These results are consistent with the results shown in Figure 2C. To visualize existing HaloTag-LA and newly synthesized HaloTag-LA simultaneously, we omitted the treatment of the cells with CHX and first labeled the cells with Halo-JF549 for 30 min. At different periods post Halo-JF549 labeling, the cells were treated with Halo Oregon Green to label newly synthesized HaloTag-LA (Figure 3A). As shown in Figure 3C, the existing HaloTag-LA was efficiently labeled by Halo-JF549. No green signal was present at 0 min post Halo-JF549 labeling. On the other hand, weak but visible newly synthesized HaloTag was detected at 15 min post-Halo-JF549 treatment. By 1 h or longer, prominent newly synthesized HaloTag-LA was detected. The newly synthesized HaloTag-LA was localized in the nucleus. These results suggest that HaloTag-LA is constantly being made in the cells and once made, it is quickly translocated into the nucleus under these conditions.

https://doi.org/10.1021/jacsau.4c00461
JACS Au 2024, 4, 3146−3156

LBL1 Induces Oligomerization of LA (1−387)

With the system to differentiate existing HaloTag-LA from newly synthesized HaloTag-LA established, we employed our previously reported **LBL1** to investigate if it has a differential effect on existing LA over newly synthesized LA, a property not possible to address using previously known methods. The small molecule ligand **LBL1** (Figure 4A) selectively binds to

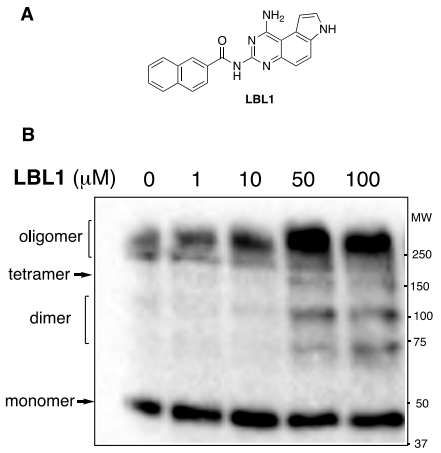

Figure 4. LBL1 induced formation of oligomeric LA (1−387). (A) Chemical structures of **LBL1**. (B) Recombinant His_6-LA (1−387) was expressed and purified from *E. coli*. The purified protein was incubated with different concentrations of **LBL1**. Then DMS was added. The sample was separated on an SDS-PAGE followed by Western blotting with anti-His antibody.

nuclear lamins in living cells.[15,16] Furthermore, we found that **LBL1** binds to LA (1−387) encompassing the nonhelical head domain and the entire helical coiled-coil rod domain.[15] As a coiled coil, LA (1−387) can exist in multiple different oligomeric states in solution. As a result, in a thermal denaturing assay, we found that LA (1−387) was melting at two distinct temperatures (T_m) with one melting at ∼40 °C (T_m1) and the other one at ∼65 °C (T_m2).[15] Interestingly, **LBL1** only shifted T_m1 without significantly affecting T_m2.[15] Based on this unique difference, we hypothesized that **LBL1** might induce formation of more oligomeric species. To test this hypothesis, we purified His-tagged LA (1−387) and investigated its oligomeric properties in the presence of **LBL1** using dimethylsuberimidate (DMS) as an amine-reactive cross-linker. DMS will react with two spatially close lysine residues.[28] In the absence of **LBL1**, the purified LA (1−387) existed as a mixture of monomer and other oligomers as evidenced by the DMS cross-linking results (Figure 4B). When LA (1−387) was incubated with **LBL1**, more dimers, tetramers, and other higher molecular weight oligomeric species of LA (1−387) were observed. These effects were dose-dependent. Interestingly, a new species at ∼75 kDa was observed. This MW is slightly less than an anticipated dimer. We interpret this as a dimer with an alternative cross-linking pattern that caused its faster migration on the SDS-PAGE gel. These results support that **LBL1** can induce formation of higher molecular weight LA assemblies. They are consistent with our earlier finding that **LBL1** only stabilized the T_m1 in the thermal shift assay and T_m1 likely reflects the melting of oligomers, whereas T_m2 indicates the melting of monomer of LA (1−387).[15]

LBL1 Differentially Modulates Newly Synthesized HaloTag-LA and Existing HaloTag-LA

To further investigate the differential properties of existing HaloTag-LA and newly synthesized HaloTag-LA in live cells, we resorted to live cell imaging enabled by the fluorescent Halo ligand (Figure 5A). We first investigated the dynamics of existing HaloTag-LA by treating the cells with CHX. Then, the cells were labeled with Halo-JF549 for live cell imaging. In the absence of **LBL1** treatment, HaloTag-LA was localized inside the nucleus with presence in both nuclear lamina and nucleoplasm (Figures 5B and S4A). The dynamics of HaloTag-LA was monitored for 3 min by capturing an image every 2 s. As expected, the HaloTag-LA signal was pretty much immobile (Figure 5B and Supplementary Movie S1). This was consistent with the FRAP results shown in Figure S3. When the cells were treated with **LBL1**, the HaloTag-LA was also predominantly present in the nucleus (Figures 5C and S4B), which is similar to the one observed without **LBL1** treatment. However, a minor population of HaloTag-LA was detected in the cytosol (red circles in Figure 5C). While the HaloTag-LA in the nucleus was essentially immobile, the minor population in the cytosol was very dynamic and moved rapidly (red circles in Figure 5C and Supplementary Movie S2).

Using the masking Halo ligand **1**, we also investigated the localization and dynamics of newly synthesized HaloTag-LA in live cells (Figure 5A, bottom). We first treated the cells with Halo ligand **1** in the absence of CHX. Then, the cells were allowed for new protein synthesis for 1 h. The newly synthesized HaloTag-LA was then labeled with Halo-JF549 for live cell imaging. As shown in Figures 5D, S4C and consistent with Figure 2C, the newly synthesized HaloTag-LA was readily detectable, albeit at lower fluorescence intensity compared to existing ones. The newly synthesized HaloTag-LA was exclusively localized in the nucleus with a prominent nuclear lamina signal, suggesting that synthesis and nuclear translocation of HaloTag-LA occurred rapidly during the 1 h period of time. In contrast to the existing HaloTag-LA, the newly synthesized HaloTag-LA displayed a few distinct characteristics. First, the newly synthesized HaloTag-LA was primarily localized at the nuclear lamina. Although nucleoplasmic HaloTag-LA was present, it was much less than what was observed with existing HaloTag-LA. Second, the localization pattern for HaloTag-LA in the nuclear lamina is less homogeneous than the existing HaloTag-LA. Third, there was apparently more aggregated HaloTag-LA, which are presented as bright dots (Figures 5D and S4C). Fourth, the newly synthesized HaloTag-LA was more mobile and dynamic than the existing HaloTag-LA (red circle and oval in Figure 5D and also Supplementary Movie S3). These features suggest that the newly synthesized HaloTag-LA has different assembly states when compared to existing HaloTag-LA in live cells.

Given these potential differences and the biochemical effect of **LBL1** on the purified LA (1−387) (Figure 4B), we anticipated that **LBL1** could have a different effect on the newly synthesized HaloTag-LA in live cells. To investigate this point, we treated the cells with **LBL1** after the existing HaloTag-LA was masked by Halo ligand **1**. Then, the newly synthesized HaloTag-LA was labeled with Halo-JF549 for live cell imaging. As presented in Figures 5E, S4D, and Supplementary Movie S4 and in stark contrast to existing HaloTag-LA, the localization pattern of newly synthesized HaloTag-LA was dramatically affected by **LBL1**. **LBL1** induced the formation of numerous HaloTag-LA aggregates

https://doi.org/10.1021/jacsau.4c00461
JACS Au 2024, 4, 3146−3156

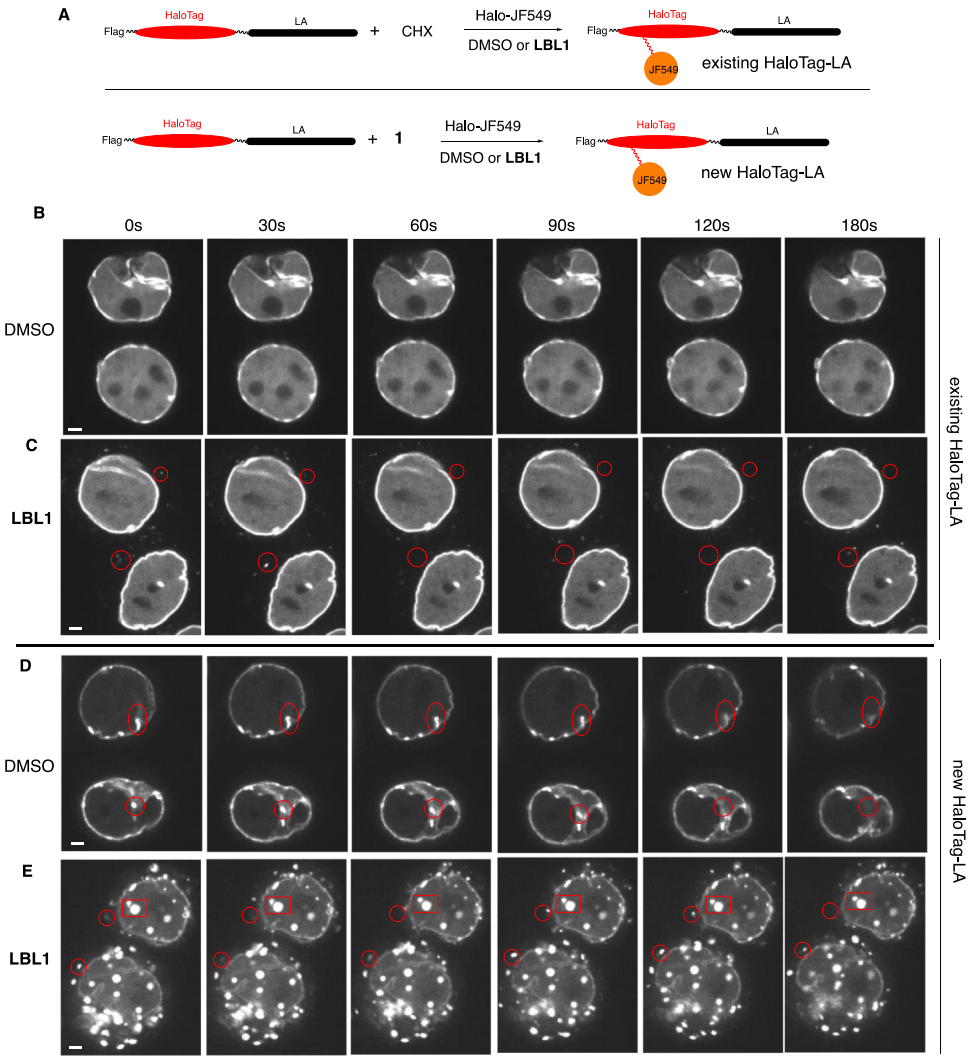

Figure 5. Live cell imaging of existing HaloTag-LA and newly synthesized HaloTag-LA using $_{CG}$-SLENP. (A) Labeling schemes to selectively label existing and newly synthesized HaloTag-LA for live cell imaging. (B, C) Live cell imaging of existing HaloTag-LA. MDA-MB-468 cells stably expressing HaloTag-LA were treated with CHX in the absence (B) or presence (C) of **LBL1**. Then HaloTag-LA was labeled with Halo-JF549. The cells were then subjected to imaging and monitored for 3 min with an image taken every 2 s. (D, E) Live cell imaging of newly synthesized HaloTag-LA. MDA-MB-468 cells stably expressing HaloTag-LA were treated with compound **1** to mask existing HaloTag-LA. Then the cells were treated with DMSO (D) or **LBL1** (E). The newly synthesized HaloTag-LA was labeled with Halo-JF549. The cells were then subjected to imaging and monitored for 3 min with an image taken every 2 s. The fluorescence display scales for each panel were adjusted differently for better clarity. The time lapse movies corresponding to each panel are provided as online Supporting Information. The scale bars are 2 μm.

both inside the nucleus and the cytosol. While the aggregates inside the nucleus were relatively immobile (red rectangle in Figure 5E), the ones in the cytosol were very mobile and dynamic (red circles in Figure 5E). Despite these changes to the aggregates in the cytosol and nucleoplasm, **LBL1** did not induce much change to the distribution of HaloTag-LA in the nuclear lamina and this pool of HaloTag-LA was also relatively immobile. We interpret the presence of cytosolic aggregates as the effect of **LBL1** being able to inhibit the nuclear translocation of lamin protein. Based on this finding, the small cytosolic aggregates present in Figure 5C might also be due to the effect of **LBL1** to block the nuclear entry of residual lamin protein molecules that were yet to reach the nucleus.

Newly Synthesized Cytosolic HaloTag-LA Colocalizes with Translating Ribosomes

Given the cytosolic localization of newly synthesized HaloTag-LA in the presence of **LBL1**, we investigated if some or all of the cytosolic aggregates of newly synthesized HaloTag-LA might still be associated with translating ribosomes. To this end, we transfected the MDA-MB-468 cells expressing HaloTag-LA with GFP-tagged ribosome protein L10 (GFP-RPL10). Then, the cells were treated with Halo ligand **1** to mask the existing HaloTag-LA. The newly synthesized HaloTag-LA was then labeled with Halo-JF549 for live cell imaging. Overexpressed ribosome protein subunits including RPL10 were reported to localize in nucleoli and cytoplasm.[29,30] In our case, we similarly observed that RPL10 was either in nucleoli or cytosol (Figure S5). When the cells were cotreated with **LBL1**, a fraction of newly synthesized HaloTag-LA was found in the cytosol. Interestingly, some of the cytosolic HaloTag-LA signals were colocalized with GFP-RPL10 (Figure S5), suggesting that this fraction of HaloTag-LA was still associated with translating ribosomes.

https://doi.org/10.1021/jacsau.4c00461
JACS Au 2024, 4, 3146−3156

CONCLUSIONS

In conclusion, we developed the first chemical genetics-based SLENP approach to selectively label newly synthesized and existing proteins. This approach is potentially generalizable to any protein of interest by creating different HaloTag in-frame fusions and the application of differentially conjugated Halo ligands. By utilizing Halo-ligands with different fluorophores, we also demonstrated that existing proteins and newly synthesized proteins can be dually labeled for visualization. Using LA as an example of filament proteins undergoing multisubunit assembly and **LBL1** as a unique small molecule to target LA, we further provide data to show that newly synthesized LA has differential susceptibility, in comparison to existing one, to small molecule ligand **LBL1**. Given the high specificity of **LBL1** for lamin labeling in cells,[16] our results indicate that the existing LA filaments do not undergo dynamic remodeling while the new ones are more susceptible to undergo dynamic remodeling and/or subunit exchange. Consistent with our in vitro cross-linking results, the newly synthesized LA proteins are likely present in a lower-order assembly state and **LBL1** can selectively induce this pool to form higher-order aggregates. These distinct aggregates are reminiscent of the aggregates formed by certain LA mutants when expressed in cells.[12,31] These results further indicate that newly synthesized LA is at least partially structured for **LBL1** binding. This is consistent with the prevailing view of folding of nascent proteins at the ribosomes.[32,33] Based on the differential effect of **LBL1**, our results indicate that newly synthesized LA is structurally different from existing LA. While the details of the differences are unknown at present, the likelihood of cotranslational assembly of LA polypeptides and their association with mRNA during nascent protein synthesis can potentially provide unique structural features that can be differentially modulated by **LBL1**. The $_{CG}$-SLENP approach described here provides a novel platform to selectively investigate the properties of newly synthesized proteins and the existing ones.

EXPERIMENTAL SECTION

Chemistry and Chemicals

The details of the synthesis of Halo ligands **1** and **2** are presented in the Supporting Information. **LBL1** was prepared according to our previously published procedure.[34] TAMRA-alkyne was obtained from Click Chemistry Tools (Scottsdale, AZ). HaloJF549, Halo Oregon Green and Halo diAcFAM were obtained from Promega (Madison, WI).

Cell Lines and Culture

HEK293T cells were purchased from ATCC. MDA-MB-468 cells were obtained from the National Cancer Institute Development Therapeutic Program. The cells were authenticated by STR profiling and tested for mycoplasm contamination by PCR. The cells were routinely cultured in high glucose Dulbecco's modified Eagle's medium (DMEM, Thermo Fisher) supplemented with 10% FBS (Hyclone) and 10% nonessential amino acids (Thermo Fisher) at 37 °C with 5% CO_2. The cells were used within 50 passages.

Plasmids and Antibodies

Flag-tagged HaloTag-LA was designed to contain N-terminal Flag tag, HaloTag, and LA. The designed in-frame fusion was assembled through gene synthesis at Genewiz (South Plainfield, NJ) and cloned into third-generation lentiviral vector pLJM1 (Addgene). GFP-RPL10 was obtained from Addgene. The following antibodies are used: mouse M2 (Sigma), mouse anti-LA (Sigma), rabbit anti-LA (Proteintech), and mouse anti-His tag (AnaSpec). Recombinant LA (1−387) was purified, as described previously.[15]

In Vitro LA (1−387) Protein Cross-Linking

His-LA (1−387) in HBS (20 mM HEPES, 250 mM NaCl, pH 8.0) (40 μg/mL) was incubated with different concentrations of **LBL1** for 1 h at room temperature. Then, dimethyl suberimidate (DMS, 11 mM) was added and the mixture was incubated at room temperature for 15 min when the cross-linking reaction was quenched with the addition of glycine (50 mM). The mixture was incubated at room temperature for 10 min. SDS-PAGE buffer was added and the sample was subjected to Western blot analysis using anti-His antibody.

Lentivirus Preparation and Transduction

The lentivirus was prepared as previously described.[35] Briefly, lentiviruses expressing HaloTag-LA were prepared from HEK 293T cells by cotransfecting lentiviral expression plasmid along with packaging vectors using the calcium-phosphate method (TaKaRa). MDA-MB-468 cells were transduced with the prepared lentiviruses expressing HaloTag-LA. After puromycin selection, the cells were used for subsequent experiments.

Confocal Microscopy

This procedure is similar to the previously published method[26] with slight modifications. MDA-MB-468 cells stably expressing HaloTag-LA and parental MDA-MB-468 cells were cultured in DMEM with 10% FBS. Once the cells reached ∼80% confluence, they were harvested and transferred to coverslips, which were coated with poly-D-lysine (R&D systems) for 24 h. For Figure 1, the cells were then treated with 2 μM Halo-JF549 for 15 min. The labeling media were removed and the cells were washed once with fresh media. Then, the cells were fixed using 4% paraformaldehyde in PBS for 15 min at room temperature followed by 10 min permeabilization with 0.3% triton X-100 in PBS at room temperature. Then, the cells were blocked in 3% BSA in PBS for 1 h at room temperature followed by overnight incubation with rabbit anti-LA antibody (1:800 in PBS with 3% BSA) at 4 °C. The next day cells were stained with a secondary Alexa fluor 488 conjugated anti-rabbit antibody (Jackson ImmunoResearch Laboratories) for 1 h at room temperature. For Figure S2, after fixation, the cells were blocked in 3% BSA in PBS for 1 h at room temperature followed by overnight incubation with rabbit anti-LA antibody (1:800 in PBS with 3% BSA) and mouse M2 (1:500 in PBS with 3% BSA) at 4 °C. The next day, the cells were stained with a secondary Alexa fluor 555 conjugated anti-rabbit antibody (Invitrogen) and a secondary Alexa fluor 488 conjugated anti-mouse antibody (Jackson ImmunoResearch Laboratories) for 1 h at room temperature.The cells were further incubated with 300 nM DAPI for 10 min at room temperature. The coverslips were mounted onto glass slides. Images were taken on an inverted Zeiss LSM 980 confocal microscope.

$_{CG}$-SLENP and Click Chemistry

MDA-MB-468 cells stably expressing HaloTag-LA were treated with or without CHX (0.1 mg/mL) along with Halo ligand **1** (10 μM) for 30 min. The media were removed and the cells were washed once with media. Then, Halo ligand **2** (10 μM) was added for another 30 min of labeling. The cells were harvested and washed twice with ice-cold PBS. The cell pellets were lysed in 1%SDS in PBS with sonication. Then, an equal amount of protein lysates (∼10 μg) was clicked with TAMRA-alkyne (10 μM) and TBTA (100 μM), TCEP (1 mM), and $CuSO_4$ (1 mM) for 1.5 h at room temperature.[36] The final SDS concentration in the click reaction was ≤0.5%. Then, the proteins were separated on a 4−20% precast SDS-PAGE gel (Biorad). The gel was scanned for fluorescent signals on ChemiDoc^{MP} (Biorad). After fluorescence imaging, the gel was stained with Coomassie blue by incubating the gel in a staining solution (Coomassie Brilliant Blue R-250 (Biorad, 2.5 mg/mL) in MeOH/ddH_2O/AcOH (4.5:4.5:1)) for overnight at room temperature. The gel was then destained in MeOH/ddH_2O/AcOH (4.5:4.5:1) before imaging.

https://doi.org/10.1021/jacsau.4c00461
JACS Au 2024, 4, 3146−3156

Dual Labeling of Existing HaloTag-LA and Newly Synthesized HaloTag-LA

MDA-MB-468 cells stably expressing HaloTag-LA were plated onto coverslips coated with poly-D-lysine (R&D systems). Then, the cells were treated with or without CHX (0.1 mg/mL) along with Halo-JF549 (Promega, 500 nM) at 37 °C for 30 min, when the media were removed and the cells were washed with fresh media. At different time points post Halo-JF549 labeling, Halo Oregon Green (Promega, 250 nM) was added and incubated at 37 °C for 30 min. The media were removed and the cells were fixed with 0.2 M sucrose and 4% PFA in 1× PBS. The cells were further incubated with 300 nM DAPI for 10 min at room temperature. The coverslips were mounted onto glass slides. Images were taken on an inverted Zeiss LSM 980 confocal microscope.

$_{CG}$-SLENP for Live Cell Imaging

MDA-MB-468 cells stably expressing HaloTag-LA were cultured with FluoroBrite DMEM (Thermo Fisher) and 10% FBS. Once cells reached ∼80% confluence, they were collected and transferred to glass bottom 4-well pie dishes (Greiner Bio-One cat# 627871), which were coated with poly-D-lysine (R&D systems) for 24 h. For imaging existing HaloTag-LA, the cells were treated with CHX (100 μg/mL) for 1 h. Then, DMSO or **LBL1** (10 μM) was added for 1 h. This was then followed by a 15 min treatment with 2 μM of Halo-JF549 ligand (Promega). Afterward, the labeling media were removed and fresh media containing DMSO or **LBL1** (10 μM) were added. The cells were then subjected to live cell microscopic imaging. Live cell imaging was performed using an inverted Nikon TiE microscope equipped with a Yokogawa CSU-W1 spinning disk confocal head, running with NIS Elements software (Nikon). The cells were maintained at 34.5 °C and 5% CO_2. Images were acquired with a Zyla v5.5 sCMOS camera (Andor) with a 100× (NA 1.49) objective. The Halo-JF549 was excited with a 561 nm laser and emission light was collected between 570 and 640 nm. A single image was taken every two seconds during each 3 min time-lapse movie. For imaging newly synthesized HaloTag-LA, the cells were treated with compound **1** (10 μM) for 30 min, when the cells were washed six times with media containing DMSO or **LBL1** (10 μM) and then incubated in media containing DMSO or **LBL1** (10 μM) for 1 h. Next, the cells were labeled with 2 μM of Halo-JF549 for 15 min. The labeling media were removed and fresh media containing DMSO or **LBL1** (10 μM) were added. The cells were then subjected to live cell microscopic imaging as above.

Colocalization of GFP-RPL10 with Newly Synthesized HaloTag-LA

MDA-MB-468 cells stably expressing HaloTag-LA were transfected with 2 μg GFP-RPL10 for 24 h. Then, the cells were transferred to glass bottom 24-well plates for two more days before the treatment. The cells were treated with compound **1** (10 μM) for 30 min, followed by washing with fresh media and then incubation with DMSO or **LBL1** (10 μM) for 1 h. Next, the cells were labeled with 500 nM of Halo-JF549 for 1 h. Z-stacks of double-positive cells were acquired on a Zeiss Celldiscoverer 7 live-cell microscope equipped with a Hamamatsu Orca Flash 4.0 sCMOS camera using a Plan Apo 50x/1.2NA water immersion objective. Standard settings for red fluorophores (for JF594) and green fluorophores (for GFP) were used, with excitation light from a Colibri7 light source (Zeiss) and channel-specific emission filters (Semrock). Analysis was performed in Zen light (Zeiss). Single middle planes from the Z-stacks are shown.

Fluorescence Recovery after Photobleaching (FRAP)

MDA-MB-468 cells stably expressing HaloTag-LA were maintained using the same protocol as above. Two days before imaging, they were collected and transferred to glass bottom 24-well plates (Cellvis cat# P24-1.5H-N), which were coated with poly-D-lysine (R&D systems) for 24 h. The cells were first treated with CHX (100 μg/mL) for 1 h. Then, the cells were treated with Halo diAcFAM (Promega, 25 nM) at 37 °C for 1.5 h. The cells were washed three times with fresh media before imaging. Images were taken on an inverted Zeiss LSM 980 confocal microscope with live cell incubation, using an LD LCI Plan Apochromat 40x/1.2NA water immersion lens. Acquisition and bleaching were performed with a 488 nm laser, and emission light was detected with a GaAsP PMT detector. Three images were taken before bleaching. For the bleach, regions at the edge of the nucleus selected for bleaching were exposed to 50% laser power with a pixel dwell time of 10.59 μs, a laser dosage empirically determined to decrease local fluorescence by at least 50%. A control region was monitored to assess bleaching from the acquisition light. Following the bleach event, single-plane images were taken every 30 s for 15 min. The images before and after bleaching were acquired at a pixel size of 0.09 μm and a pixel dwell time of 2.65 μs using bidirectional scanning. The time series was then aligned in Zeiss Zen 3.7 to account for cell movement and allow accurate measurement of fluorescence recovery.

■ ASSOCIATED CONTENT

Supporting Information

The Supporting Information is available free of charge at https://pubs.acs.org/doi/10.1021/jacsau.4c00461.

Additional experimental procedure for the synthesis of **1** and **2**; HaloTag-LA sequence; additional confocal micrographs; FRAP data; and localization of newly synthesized HaloTag-LA and GFP-RPL10 (PDF)

Time-lapse movie of existing HaloTag-LA treated with DMSO (MP4)

Time-lapse movie of existing HaloTag-LA treated with **LBL1** (10 μM) (MP4)

Time-lapse movie of newly synthesized HaloTag-LA treated with DMSO (MP4)

Time-lapse movie of newly synthesized HaloTag-LA treated with **LBL1** (10 μM) (MP4)

■ AUTHOR INFORMATION

Corresponding Author

Bingbing X. Li − *Department of Chemical Physiology and Biochemistry, Knight Cancer Institute, Oregon Health & Science University, Portland, Oregon 97239, United States;* orcid.org/0000-0001-8259-9448; Email: lib@ohsu.edu

Authors

Jian Wang − *Department of Chemical Physiology and Biochemistry, Oregon Health & Science University, Portland, Oregon 97239, United States;* orcid.org/0000-0003-0806-9590

Bo Chao − *Department of Chemical Physiology and Biochemistry, Oregon Health & Science University, Portland, Oregon 97239, United States;* orcid.org/0000-0002-4186-8354

Jake Piesner − *Department of Chemical Physiology and Biochemistry, Oregon Health & Science University, Portland, Oregon 97239, United States*

Felice Kelly − *Advanced Light Microscopy Shared Resource, Oregon Health & Science University, Portland, Oregon 97239, United States*

Stefanie Kaech Petrie − *Department of Neurology, Knight Cancer Institute, Oregon Health & Science University, Portland, Oregon 97239, United States*

Xiangshu Xiao − *Department of Chemical Physiology and Biochemistry, Knight Cancer Institute, Oregon Health & Science University, Portland, Oregon 97239, United States;* orcid.org/0000-0001-9520-1371

Complete contact information is available at: https://pubs.acs.org/10.1021/jacsau.4c00461

Author Contributions

CRediT: **Jian Wang** data curation, methodology, writing-original draft, writing-review & editing; **Bo Chao** data curation, methodology, writing-review & editing; **Jake Piesner** methodology, writing-review & editing; **Felice Kelly** formal analysis, methodology, visualization, writing-review & editing; **Stefanie Kaech Petrie** formal analysis, methodology, writing-review & editing; **Xiangshu Xiao** conceptualization, data curation, formal analysis, funding acquisition, investigation, methodology, project administration, supervision, validation, writing-original draft, writing-review & editing; **Bingbing X Li** conceptualization, data curation, formal analysis, funding acquisition, investigation, methodology, project administration, resources, software, supervision, validation, visualization, writing-original draft, writing-review & editing.

Notes

The authors declare no competing financial interest.

■ ACKNOWLEDGMENTS

This work was made possible by financial support provided from R21EB028425 (BXL), R01CA245964 (BXL), R01CA278058 (BXL and XX), R01CA211866 (XX), and R01GM122820 (XX). We thank OHSU Gene Profiling Shared Resource for authenticating the cell lines through STR profiling and OHSU Advanced Light Microscopy Shared Resource for providing technical support. The OHSU Advanced Light Microscopy Shared Resource and Gene Profiling Shared Resource were partially supported by P30CA069533.

■ REFERENCES

(1) Ahnert, S. E.; Marsh, J. A.; Hernández, H.; Robinson, C. V.; Teichmann, S. A. Principles of assembly reveal a periodic table of protein complexes. *Science* **2015**, *350* (6266), No. aaa2245.

(2) Schwarz, A.; Beck, M. The Benefits of Cotranslational Assembly: A Structural Perspective. *Trends Cell Biol.* **2019**, *29* (10), 791−803.

(3) Duncan, C. D.; Mata, J. Widespread cotranslational formation of protein complexes. *PLoS Genet* **2011**, *7* (12), No. e1002398.

(4) Natan, E.; Wells, J. N.; Teichmann, S. A.; Marsh, J. A. Regulation, evolution and consequences of cotranslational protein complex assembly. *Curr. Opin. Struct. Biol.* **2017**, *42*, 90−97.

(5) Pegoraro, A. F.; Janmey, P.; Weitz, D. A. Mechanical Properties of the Cytoskeleton and Cells. *Cold Spring Harb. Perspect. Biol.* **2017**, *9* (11), No. a022038.

(6) Dechat, T.; Adam, S. A.; Taimen, P.; Shimi, T.; Goldman, R. D. Nuclear lamins. *Cold Spring Harb. Perspect. Biol.* **2010**, *2* (11), No. a000547.

(7) Dechat, T.; Pfleghaar, K.; Sengupta, K.; Shimi, T.; Shumaker, D. K.; Solimando, L.; Goldman, R. D. Nuclear lamins: major factors in the structural organization and function of the nucleus and chromatin. *Genes Dev.* **2008**, *22* (7), 832−53.

(8) Burke, B.; Stewart, C. L. The nuclear lamins: flexibility in function. *Nat. Rev. Mol. Cell Biol.* **2013**, *14* (1), 13−24.

(9) Aebi, U.; Cohn, J.; Buhle, L.; Gerace, L. The nuclear lamina is a meshwork of intermediate-type filaments. *Nature* **1986**, *323* (6088), 560−4.

(10) Turgay, Y.; Eibauer, M.; Goldman, A. E.; Shimi, T.; Khayat, M.; Ben-Harush, K.; Dubrovsky-Gaupp, A.; Sapra, K. T.; Goldman, R. D.; Medalia, O. The molecular architecture of lamins in somatic cells. *Nature* **2017**, *543* (7644), 261−264.

(11) Turgay, Y.; Medalia, O. The structure of lamin filaments in somatic cells as revealed by cryo-electron tomography. *Nucleus* **2017**, *8* (5), 475−481.

(12) Loewinger, L.; McKeon, F. Mutations in the nuclear lamin proteins resulting in their aberrant assembly in the cytoplasm. *EMBO J.* **1988**, *7* (8), 2301−9.

(13) Kamenova, I.; Mukherjee, P.; Conic, S.; Mueller, F.; El-Saafin, F.; Bardot, P.; Garnier, J. M.; Dembele, D.; Capponi, S.; Timmers, H. T. M.; Vincent, S. D.; Tora, L. Co-translational assembly of mammalian nuclear multisubunit complexes. *Nat. Commun.* **2019**, *10* (1), 1740.

(14) Lautier, O.; Penzo, A.; Rouvière, J. O.; Chevreux, G.; Collet, L.; Loïodice, I.; Taddei, A.; Devaux, F.; Collart, M. A.; Palancade, B. Co-translational assembly and localized translation of nucleoporins in nuclear pore complex biogenesis. *Mol. Cell* **2021**, *81* (11), 2417.e5−2427.e5.

(15) Li, B. X.; Chen, J.; Chao, B.; David, L. L.; Xiao, X. Anticancer pyrroloquinazoline LBL1 targets nuclear lamins. *ACS Chem. Biol.* **2018**, *13*, 1380−1387.

(16) Li, B. X.; Chen, J.; Chao, B.; Zheng, Y.; Xiao, X. A Lamin-Binding Ligand Inhibits Homologous Recombination Repair of DNA Double-Strand Breaks. *ACS Central Science* **2018**, *4* (9), 1201−1210.

(17) Bonifacino, J. S. Metabolic labeling with amino acids. *Curr. Protoc. Cell Biol.* **2001**, *Chapter 7*, No. Unit 7.1, DOI: 10.1002/0471143030.cb0701s00.

(18) Dieterich, D. C.; Link, A. J.; Graumann, J.; Tirrell, D. A.; Schuman, E. M. Selective identification of newly synthesized proteins in mammalian cells using bioorthogonal noncanonical amino acid tagging (BONCAT). *Proc. Natl. Acad. Sci. U. S. A.* **2006**, *103* (25), 9482−7.

(19) England, C. G.; Luo, H.; Cai, W. HaloTag technology: a versatile platform for biomedical applications. *Bioconjugate Chem.* **2015**, *26* (6), 975−86.

(20) Shimi, T.; Kittisopikul, M.; Tran, J.; Goldman, A. E.; Adam, S. A.; Zheng, Y.; Jaqaman, K.; Goldman, R. D. Structural organization of nuclear lamins A, C, B1, and B2 revealed by superresolution microscopy. *Mol. Biol. Cell* **2015**, *26* (22), 4075−86.

(21) Jagatheesan, G.; Thanumalayan, S.; Muralikrishna, B.; Rangaraj, N.; Karande, A. A.; Parnaik, V. K. Colocalization of intranuclear lamin foci with RNA splicing factors. *J. Cell Sci.* **1999**, *112* (Pt 24), 4651−4661.

(22) Karoutas, A.; Szymanski, W.; Rausch, T.; Guhathakurta, S.; Rog-Zielinska, E. A.; Peyronnet, R.; Seyfferth, J.; Chen, H. R.; de Leeuw, R.; Herquel, B.; Kimura, H.; Mittler, G.; Kohl, P.; Medalia, O.; Korbel, J. O.; Akhtar, A. The NSL complex maintains nuclear architecture stability via lamin A/C acetylation. *Nat. Cell Biol.* **2019**, *21* (10), 1248−1260.

(23) Rostovtsev, V. V.; Green, L. G.; Fokin, V. V.; Sharpless, K. B. A stepwise huisgen cycloaddition process: copper(I)-catalyzed regioselective "ligation" of azides and terminal alkynes. *Angew. Chem., Int. Ed. Engl.* **2002**, *41* (14), 2596−9.

(24) Murrey, H. E.; Judkins, J. C.; Am Ende, C. W.; Ballard, T. E.; Fang, Y.; Riccardi, K.; Di, L.; Guilmette, E. R.; Schwartz, J. W.; Fox, J. M.; Johnson, D. S. Systematic Evaluation of Bioorthogonal Reactions in Live Cells with Clickable HaloTag Ligands: Implications for Intracellular Imaging. *J. Am. Chem. Soc.* **2015**, *137* (35), 11461−75.

(25) Obrig, T. G.; Culp, W. J.; McKeehan, W. L.; Hardesty, B. The mechanism by which cycloheximide and related glutarimide antibiotics inhibit peptide synthesis on reticulocyte ribosomes. *J. Biol. Chem.* **1971**, *246* (1), 174−81.

(26) Xiao, X.; Li, B. X. Identification of lamins as the molecular targets of LBL1 using a clickable photoaffinity probe. *Methods Enzymol.* **2020**, *633*, 185−201.

(27) Moir, R. D.; Yoon, M.; Khuon, S.; Goldman, R. D. Nuclear lamins A and B1: different pathways of assembly during nuclear envelope formation in living cells. *J. Cell Biol.* **2000**, *151* (6), 1155−68.

(28) Packman, L. C.; Perham, R. N. Quaternary structure of the pyruvate dehydrogenase multienzyme complex of Bacillus stearothermophilus studied by a new reversible cross-linking procedure with bis(imidoesters). *Biochemistry* **1982**, *21* (21), 5171−5.

https://doi.org/10.1021/jacsau.4c00461
JACS Au 2024, 4, 3146−3156

(29) Lam, Y. W.; Lamond, A. I.; Mann, M.; Andersen, J. S. Analysis of nucleolar protein dynamics reveals the nuclear degradation of ribosomal proteins. *Curr. Biol.* **2007**, *17* (9), 749−60.
(30) Heiman, M.; Schaefer, A.; Gong, S.; Peterson, J. D.; Day, M.; Ramsey, K. E.; Suárez-Fariñas, M.; Schwarz, C.; Stephan, D. A.; Surmeier, D. J.; Greengard, P.; Heintz, N. A translational profiling approach for the molecular characterization of CNS cell types. *Cell* **2008**, *135* (4), 738−48.
(31) Piekarowicz, K.; Machowska, M.; Dratkiewicz, E.; Lorek, D.; Madej-Pilarczyk, A.; Rzepecki, R. The effect of the lamin A and its mutants on nuclear structure, cell proliferation, protein stability, and mobility in embryonic cells. *Chromosoma* **2017**, *126* (4), 501−517.
(32) Thommen, M.; Holtkamp, W.; Rodnina, M. V. Co-translational protein folding: progress and methods. *Curr. Opin. Struct. Biol.* **2017**, *42*, 83−89.
(33) Kramer, G.; Shiber, A.; Bukau, B. Mechanisms of Cotranslational Maturation of Newly Synthesized Proteins. *Annu. Rev. Biochem.* **2019**, *88*, 337−364.
(34) Chen, J.; Kassenbrock, A.; Li, B. X.; Xiao, X. Discovery of a Potent Anti-tumor Agent through Regioselective Mono–acylation of 7-Pyrrolo[3,2-]quinazoline-1,3-diamine. *Medchemcomm* **2013**, *4* (9), 1275−1282.
(35) Li, B. X.; David, L. L.; Davis, L. E.; Xiao, X. Protein arginine methyltransferase 5 is essential for oncogene product EWSR1-ATF1-mediated gene transcription in clear cell sarcoma. *J. Biol. Chem.* **2022**, *298* (10), No. 102434.
(36) Martín-Acosta, P.; Meng, Q.; Klimek, J.; Reddy, A. P.; David, L.; Petrie, S. K.; Li, B. X.; Xiao, X. A clickable photoaffinity probe of betulinic acid identifies tropomyosin as a target. *Acta Pharmaceutica Sinica B* **2022**, *12* (5), 2406−2416.

https://doi.org/10.1021/jacsau.4c00461
JACS Au 2024, 4, 3146−3156